Colloid Polym Sci (2007) 285:413–421
DOI 10.1007/s00396-006-1583-7

ORIGINAL CONTRIBUTION

Colloidal nanocomposite hydrogel particles

Nurettin Sahiner

Received: 17 July 2006 / Accepted: 5 September 2006 / Published online: 3 November 2006

Abstract Quaternary ammonium salt, (3-acrylamidopropyl)-trimethylammonium chloride was used to synthesize nanohydrogel and composite particles such as inorganic–organic hybrid composites and hydrogel nanoparticles with magnetic properties utilizing a water-in-oil microemulsion system. The positively charged cationic monomer was chosen to promote silica hydrolysis and condensation to prepare silica-hydrogel nanocomposite particles with interesting morphologies. It was shown that highly monodisperse, completely charged nanohydrogel can be used to encapsulate ferrite particles. Furthermore, it was also confirmed that cationic nanohydrogel particles with variant morphology can be prepared by employing suitable silica precursor. Morphology, structure, properties, and size of nanocomposite materials were explored utilizing transmission electron microscopy, atomic force microscopy, and vibrating sample magnetometer.

Keywords Nanogel · Nanocomposite · Magnetic field responsive hydrogel · Polymeric biomaterials · Silica-hydrogel · Ceramic-nanogel

N. Sahiner (✉)
Faculty of Science, Chemistry Department,
Canakkale Onsekiz Mart University,
Terzioglu Campus,
Canakkale 17020, Turkey
e-mail: sahiner@udel.edu

Present address:
N. Sahiner
Materials Science and Engineering, University of Delaware,
201 DuPont Hall,

Introduction

To prepare novel materials, a variety of templates can be used [1]. For example, materials with desired properties have been obtained by utilizing the geometrically confined spaces [2] such as surfactants [3], block copolymers [4], self-assembly [5], multiple layers of sequentially adsorbed polyelectrolytes [6] or layer-by-layer polyionic assemblies [7], and polymeric micelles including reverse micelles [8–12].

Hydrogels have found numerous uses ranging from daily life applications, mainly due to their high water absorption capacity (e.g., cosmetics and personal care products), to the development and implementation of new environmentally responsive materials for biological applications [13–15]. Hydrogels are inherently soft, hydrophilic, porous, and elastic, which are prerequisites for many biological applications as scaffolds in cell growing media and tissue engineering, drug delivery vehicles for control and guided release of active agents, and imaging technologies [16–20]. Because of the complex, diverse, and challenging environments of biological systems, materials that can be used in this field should be proficient and have tunable characteristics. Hydrogels, in that respect, are viable materials that can execute specific functions by design and are manipulatable. The combination of a responsive hydrogel with a rigid porous supporting structure yields a membrane with high mechanical strength and a high on–off-permeability ratio [21]. A new concept for a mechanically stable drug release system is to combine hydrogels with porous inorganic or ceramic membranes to support the delicate responsive hydrogel as a partner. It has been reported that hybrid nanogels synthesized by incorporating the polymer into a tailored nanostructure, ceramic hosts, or vice versa, provide more uniform release rate of drugs, as well as a sustained release profile [22, 23]. Hydrogels can further be

made magnetic-field-responsive due to the potential applications of magnetic gels in magnetic drug delivery, cell sorting, catalysis, sensors, and actuators [24–26]. For a specific purpose, molecular receptors can be attached to the nanoparticles to render specific recognition features with controllable porosity. The integration of the nanoparticles with polymeric hydrogels facilitates the ways to design signal-triggered materials with novel electronic properties [27]. Tailored magnetic bulk, micro- and nanoparticles have recently been receiving growing attention because of their extensive applications in the fields of biology and medicine, such as protein and enzyme immobilization, bioseparation, immunoassays, hyperthermia, and controlled drug delivery [24, 28, 29]. By definition, ferrogel contains ferromagnetic fluid or finely distributed ferromagnetic particles, which are attached to the flexible network chains by adhesive forces giving rise to direct coupling between the magnetic and mechanical properties of both materials. Colloidal dispersion of monosized magnetic particles with a typical size of below 10 nm or a ferrofluid within a crosslinked polymer network endow superparamagnetic behavior [30], the same as ferromagnetic fluids. On the other hand, particles with diameters of about 100 nm or larger correspond to ferromagnetism [31].

Here, a method is described by utilizing water-in-oil microemulsion system for syntheses of composite materials. A cationic monomer was used for nanohydrogel nanocomposite preparation because it is positively charged and pH responsive and, therefore, can be exploited further for inorganic–organic nanocomposite synthesis. These types of monomers can facilitate the silica hydrolysis and condensation reaction to prepare interesting colloidal ceramic composite materials with intriguing morphology and characteristics. Moreover, iron particles (ferrites) were encapsulated with cationic nanohydrogel matrix in situ with the same synthesis method.

Experimental

Materials

(3-Acrylamidopropyl)-trimethylammonium chloride (APTMACl), acrylamide (AAm) as monomers, *N*,*N*′-methylenebisacrylamide (Bis) as a crosslinker (X), ammonium persulfate (APS) as redox initiator, *N*,*N*,*N*′,*N*′-tetramethylethylenediamine (TEMED) as an accelerator, dioctyl sulfosuccinate sodium salt (AOT) as surfactant, 2,2,4-trimethylpentane (isooctane) as organic solvent, and 2,2′-azobisisobutyronitrile as a radical initiator were used. Metal ion source was $FeSO_4.7H_2O$, and NH_4OH was used as precipitating agent. Tetramethoxylsilane (TMOS), tetraethoxysilane (TEOS), vinyltrimethoxysilane (VTMOS), and vinyltriethoxysilane (VTEOS) were used as silica precursors. All the reagents were of analytical grade or the highest purity available, used without further purification, and purchased from Aldrich Chemical (Milwaukee, WI, USA).

Nanogel and hybrid organic–inorganic nanocomposite synthesis

Nanogels of APTMACl were synthesized in inverse microemulsion system at ambient temperature by redox polymerization method. The polymerization was carried out at w_0=10 (w_0=H2O/[AOT]) medium with various amounts of X ratios. The synthesis of nanogels was accomplished by modifying the previously reported procedure [32]. In a typical route, 0.1 ml of APTMACl was mixed with the crosslinker solution, which was previously prepared with varying amounts of X (0.5–5 mol%) in the presence of 10 μl TEMED and transferred to a 20 ml container containing 15 ml 0.1 M AOT solution in isooctane. This solution was vortex-stirred to obtain clear water-in-oil microemulsion. After mixing all these components, the mixture was purged with nitrogen for at least 1 min to remove the dissolved oxygen, followed by the addition of the initiator solution, 1% (with respect to monomer amount) and another 5 μl of TEMED was added. The total water level was adjusted to bring the final water content w_0=10 condition with initiator solution. The simultaneous polymerization and crosslinking reaction was carried out for 24 h with continuous stirring on a magnetic stirrer set up at ambient temperature. After reaction, the mixture remains clear, indicating that any crosslinked polymer formed remains sustained in the microemulsion droplets. The nanogel was then precipitated using excess acetone to destabilize the micelles. Several centrifugation and washing procedures were employed to virtually remove the surfactant. The usage of AAm as a comonomer (one-to-one mole ratio with respect to APTAMCl) also provides copolymeric nanohydrogels that afford rigidity to the network and the ability to control the charge extent in the structure.

To prepare hybrid organic–inorganic composite materials with cationic monomer, various silica precursors, such as TMOS, TEOS, and vinyl group containing precursors, VTMOS and VTEOS, were utilized. For the hybrid material synthesis, the same system, water-in-oil micro emulsion, was employed. The typical composite materials synthesis with TMOS is as follows: to the water-in-oil microemulsion, 15 ml 0.1 M AOT in isooctane containing all the components for cationic hydrogel synthesis with the exception of the APS, were added various mole ratios of silica precursor, i.e., TMOS/APTMACl (0.5:1, 1:1, 1:2, and 4:1). The reaction was preceded for 2 h, followed by addition of aqueous solution initiator (0.5% with respect to monomer amount) for the polymerization-crosslinking

reaction. The mixture was stirred for another 24 h to complete the composite synthesis. This method was also engaged with vinyl group containing silica precursors for organic–inorganic hybrid materials synthesis.

Ferrite particle encapsulated nanocomposite synthesis

Magnetic particles encapsulated by hydrogels were prepared with a two-step approach. In the first step, the iron particles were prepared with a method reported previously [33]. In that method, aqueous $FeSO_4$ containing AOT reverse micelle solution (w_0=10) was prepared in 7.5 ml 0.5 M AOT in isooctane. To this solution was added an equal amount of another similarly prepared AOT reverse micelle solution containing NH_4OH, obtained from ~30% aqueous NH_4OH with w_0=10 in 0.5 M AOT in isooctane. After vigorous stirring for 2 h at ambient temperature, the isooctane and water were removed through evacuation in a vacuum oven at 50 °C for 24 h, leading to a dry residue of ferrite particles stabilized with AOT surfactants. Subsequent to formation of ferrite particle, the AOT reverse micelles containing these ferrite particles were reconstituted with hydrogel precursors (monomer, crosslinker, and accelerator). Followed by addition of initiator solution to satisfy the w_0=10 conditions as described previously, the polymerization was carried out again 24 h at ambient temperature. For the removal of surfactant, the same procedure was followed as is in cationic nanohydrogel synthesis, in which acetone was chosen as solvent, which is a good solvent for surfactant (AOT) and a precipitant for the cationic hydrogels. The crosslinker used in the encapsulation of ferrite particle was relatively higher (2–5%) to prevent the leaking out of iron particles from the nanogel network. Additionally, AAm was also used to ensure that no leakage of iron particles from the network could occur.

Nanocomposite characterization

For the morphological and size determination, nanoparticles were imaged using transmission electron microscopy (TEM) and atomic force microscopy (AFM). For TEM imaging of the nanoparticles, a drop of aliquot was taken after completion of reactions and diluted 60–80-fold with isooctane and placed on a formvar-coated copper TEM grid and dried in a closed environment at ambient temperature for at least 12 h before imaging. TEM micrographs were

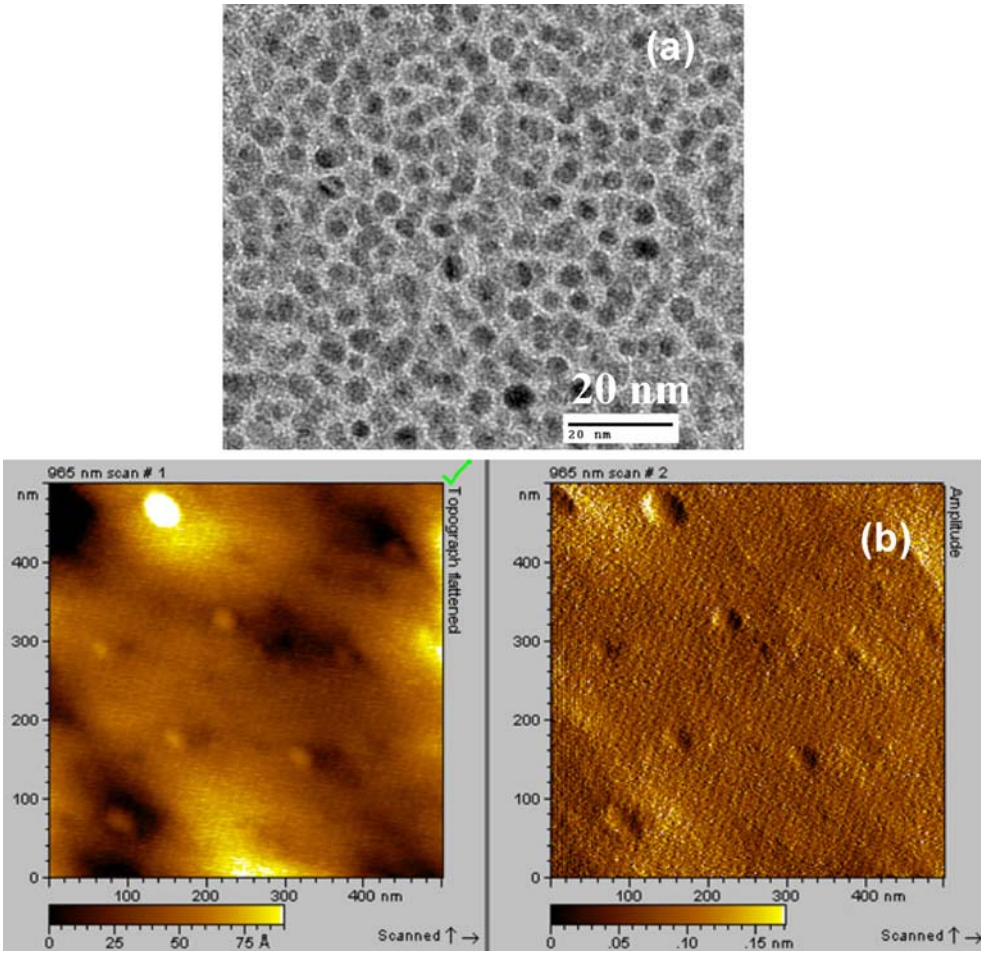

Fig. 1 TEM (**a**) and AFM (**b**) images of 1% crosslinked (1% X) cationic p(APTMACl) hydrogels

acquired using a JEOL (Tokyo, Japan) JEM 2010 electron microscope operating at 200 kV. For AFM measurements (I-MAC Molecular Imaging, San Diego, CA, USA), purified nanoparticles were diluted and swollen in distilled water, and a drop of swollen nanogel was placed on the mica surface and dried in the closed environment at ambient temperature, again for at least 12 h. It was observed that the intermittent contact mode (tapping mode) technique was capable of imaging the polymeric nanoparticles. Magnetic properties of the synthesized materials were investigated using vibrating sample magnetometer (VSM).

Results and discussion

The cationic monomer, APTMACl, chosen in this study is an AAm derivative and can be polymerized by UV irradiation or redox polymerization method [34]. For nanomaterial synthesis, the reverse micelle technique is one of the most frequently applied methods [35, 36]. Figure 1a and b shows the TEM and AFM images of cationic nanohydrogel obtained from the AOT reverse micellar systems, respectively. The nanohydrogel particles obtained by this method are about 5 nm in diameter and almost uniform in size in dried state, as seen from TEM image. AFM images, on the other hand, depict slightly larger particle sizes of about 20–40 nm. The positively charged cationic hydrogels, swollen in water, stick on the mica surface due to the electrostatic interaction between charges of nanogels (positive) and the mica surface (negative). Additionally, as reported by DeSimone et al., the interaction between the AFM tip and the nanoparticles results in the measurement of bigger particle sizes [37].

Figure 2 denotes a scheme of the possibility of designing a system that can encapsulate nanohydrogel and/or incorporate polymer into a tailored nanostructure ceramic host or vice versa. Combining inorganic properties with responsive hydrogel material could offer new opportunities; for example, improved mechanical/structural integrity can be obtainable while affording flexible and functional polymer chains, which are very essential in biological applications. To synthesize ceramic composite material, two approaches were employed. In the first approach, silica precursor, such as TMOS or TEOS, was used to prepare amorphous silica in the reverse micelles of AOT, which has appropriate conditions for hydrolysis and condensation reactions. In the second one, a polymerizable functional group containing silica precursors such as VTMOS or VTEOS was dissolved in the AOT system, which already contains APTMACl hydrogel precursor and water. The AMPTACl is chosen intentionally because its aqueous monomer solution has already sufficient pH value (~9.5) for promoting silica hydrolysis and condensation. It is known that in proper

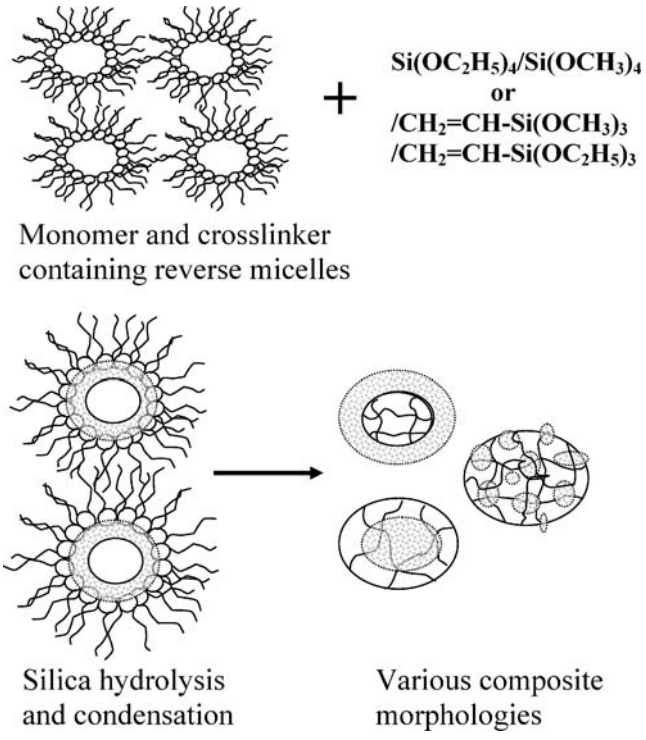

Fig. 2 Synthesis scheme of organic–inorganic nanocomposites with the utilization of various silica precursors

acidic or basic conditions, silica particles can be prepared with various morphologies [38–40]. The reverse micelles contain hydrogel precursors (dispersed aqueous phase in oil), while the silica precursor are partitioning in the oil phase of AOT solution (in isooctane). With the continuous stirring during the reaction, silica precursors migrate to the periphery of the reverse micelles, which already has proper conditions for hydrolysis and condensation (water and basic pH). By the addition of initiator, polymerization-crosslinking and silica hydrolysis-condensations can concurrently or consecutively be accomplished.

In Fig. 3, the TEM images of ceramic-hydrogel composites obtained with TMOS silica precursor are shown. It was observed that the reactions of TMOS and VTMOS for the nanocomposites synthesis were faster than their corresponding ethoxy counterparts by trial and error. In Fig. 3, the mole ratios of TMOS to APTMACl were varied and depicted in the following order: 0.5 (Fig. 3a), 1 (Fig. 3b), 2 (Fig. 3c), and 4 (Fig. 3d). As can be seen from the images, with the increase in the amount of silica precursors, there is distortion in the shape of the composite particles. This can be explained by the interdroplet collision during the condensation reaction. The reverse micelles are in dynamic equilibrium and the increase in the amount of silica precursors increases the chances of growing silica particles collision and condensation at the periphery of reverse micelles, resulting in variations in the shapes of the

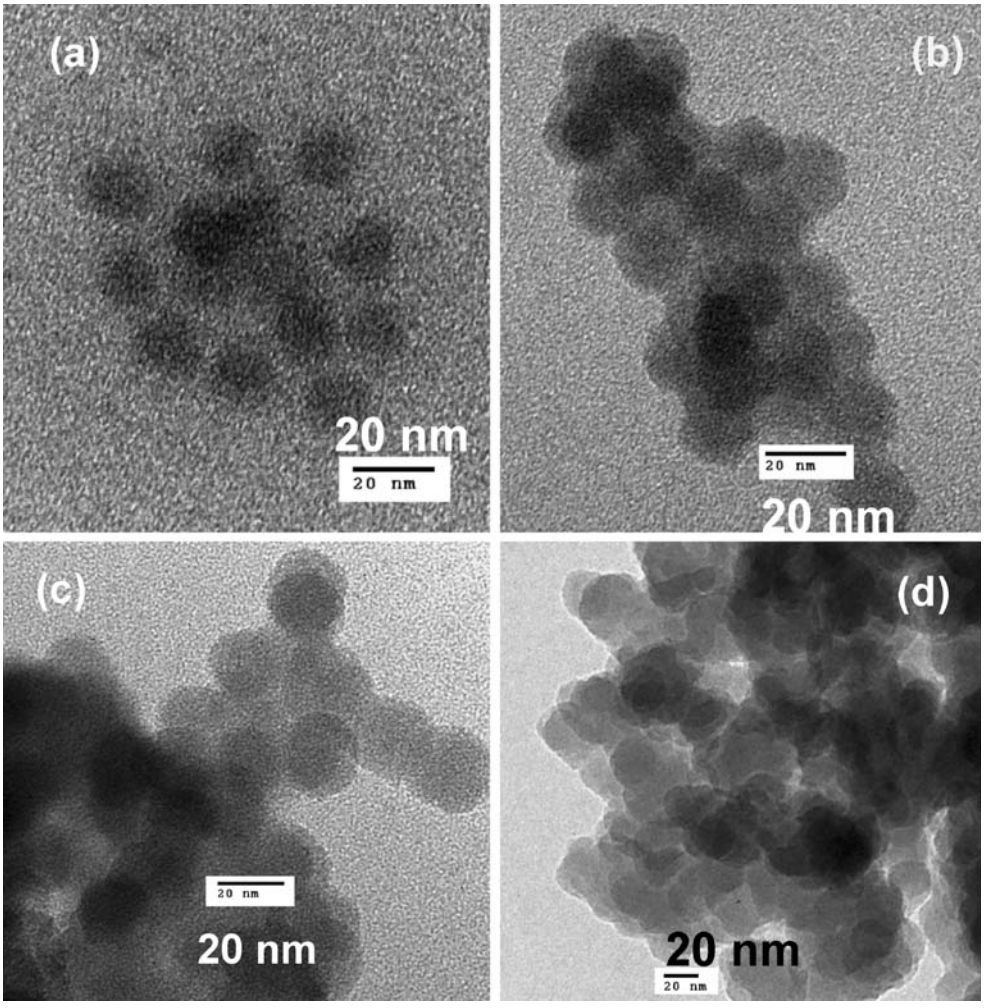

Fig. 3 Inorganic–organic hydrogel nanocomposites prepared with TMOS in mole ratios to cationic APTMACl monomer of 0.5 (**a**), 1 (**b**), 2 (**c**), and 4 (**d**)

composite materials. As depicted in Fig. 2, various morphological structures can be obtained by the appropriate choice of ceramic precursors. Instead of encapsulation silica particles inside cationic hydrogels, silica particles can also be chemically anchored to the hydrogel matrix by using vinyl group containing silica precursors, such as VTMOS and VTEOS.

Figure 4 illustrates the TEM images of organic–inorganic composite materials obtained by utilizing VTMOS with a one-to-one mole ratio to cationic monomer. In the close-up image of Fig. 4b, the black dots can be clearly seen. These darker spot can be assigned to condensed silica particles anchored to the hydrogel matrix via covalent bonding from its vinyl functionality. As revealed from these TEM images, it is possible to engineer composite nanostructures with an appropriate choice material. For example, hydrogels are soft, porous, and responsive materials, while silica particles are mechanically stronger but brittle and have well-defined structural properties. In this perspective, the combination of these two materials provides materials with tunable properties for unique applications in nanoscale. For instance, mechanical and permeation properties can be optimized almost independently over a large range of parameters for the separation or recognition of certain molecules. The grafting of hydrogels on the surface of cylindrical pores or insertion of solid structure into a matrix afford a nanomesh, which can control the effective pore size by shrinking or swelling according to the environmental factors that effect hydrogel swelling, shrinking, bending, degrading, or curling.

Other kinds of nanocomposite materials, for example, enhanced composites (responsive to more than one stimulus), can be synthesized by coating magnetic metal particles with a functional polymer matrix, which is also stimuli-sensitive, e.g., pH, temperature, solute molecules, ionic strength of the medium, and so on. Figure 5 shows the schematic of iron particle encapsulation inside cationic nanohydrogels by a two-step approach. In the first step, as shown in Fig. 5a, equal volumes of ferrite particle precursors, $FeSO_4$ and NH_4OH, were mixed in an AOT reverse micelle system to form nanosized ferrite particle in water phase of the continuous oil phase. The reverse

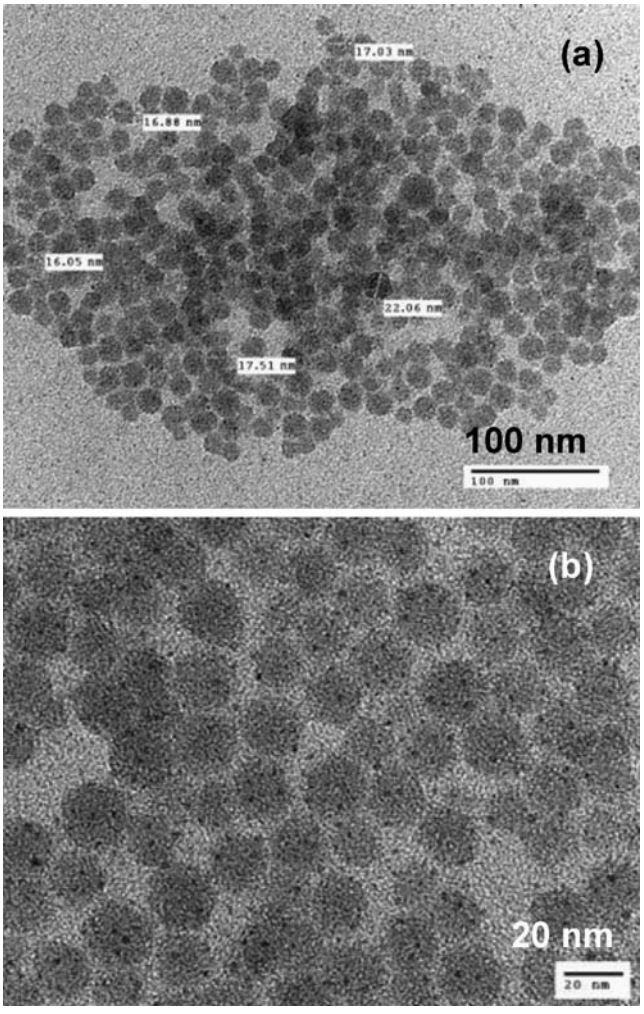

Fig. 4 Inorganic–organic hydrogel nanocomposites prepared with VTMOS with a 1:1 mole ratio to APTMACl cationic monomer (**a**), and the close-up images (**b**)

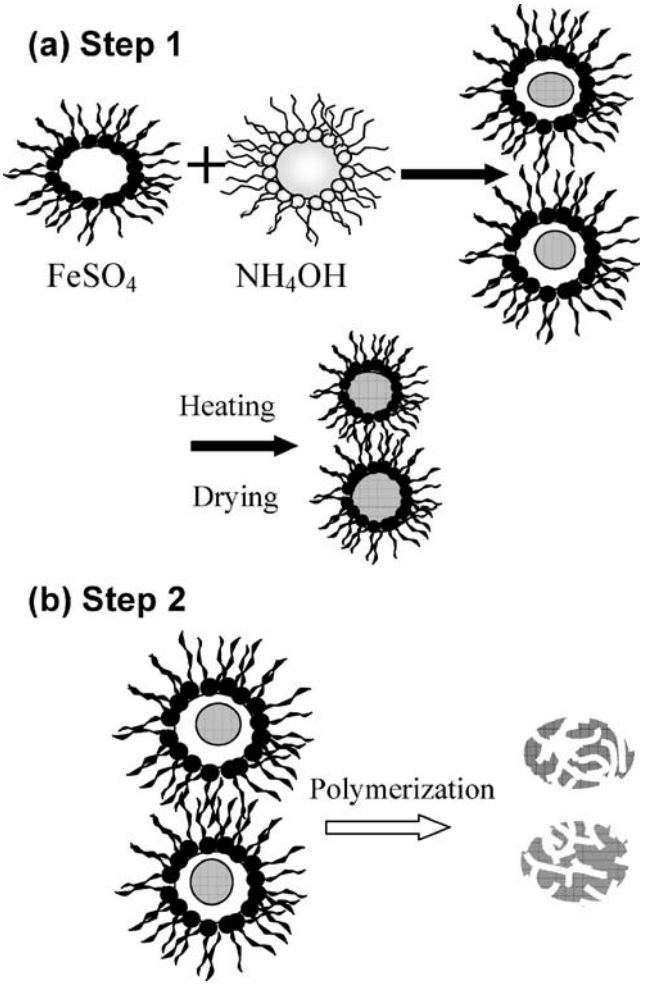

Fig. 5 Scheme of ferrite-containing composite hydrogels. **a** Ferrite particles synthesis from its reagents in AOT reverse micelles. **b** Reconstitution of magnetic particle with hydrogel precursor and simultaneous polymerization-crosslinking to encapsulate iron particles

micelles of AOT were used as nanoreactor for iron particle formation and utilized as stabilizing agent to prevent aggregation of the formed ferrite particles. Upon mixing these two precursors, an instantaneous dark mixture of greenish/brown color appears as an indication of the reaction by precipitation of ferrous hydroxide complexes. These complexes are quickly oxidized to ferric hydroxide complexes by the atmospheric oxygen. After stirring thoroughly for 2 h, the oil (isooctane) of continuous phase and the water of aqueous phase were removed in an oven by evacuation at 50 °C for 24 h to yield dried reverse micelles containing ferrous hydroxide complexes. The presence of AOT prevents further growth of ferrite particles. These dried reverse micelles were reconstituted with isooctane and aqueous cationic hydrogel precursor. The clear brown color of the mixture can be attributed to iron hydroxide complexes. The presence of ferric and ferrous hydroxide leads to the formation of magnetite or maghemite [33, 41, 42]. The suspended particle mixture was polymerized with the addition of redox initiator at ambient temperature, as depicted in Fig. 5b. The surfactant was removed by exhaustive washing with acetone and centrifugation. Here, a relatively high amount of crosslinker was used to prevent leakage of iron particles. Although the ionic hydrogels are highly water-swollen, their swelling depends on the pH and ionic strength of the medium as well as the amount of crosslinker used during the synthesis [32].

It was shown in earlier work that APTMACl gives completely three-dimensional networks above 0.5% X (crosslinker ratio with respect to monomer extent) [43]. The upper limit for crosslinker amount in this work was chosen as 5% because even this concentration causes the rupture of the structure in the bulk hydrogel prepared at the same conditions with nanogels. Due to the rigidity of the network and close proximity of the positive charges, the network expands enormously by repulsion of positive charges in distilled water, and eventually, the network loses its integrity by breaking apart into smaller pieces. It was

anticipated that 3% or greater crosslinking ratio with respect to monomer amount should prevent the leakage of iron particles. Intuitively, it is also possible that there is an attractive force between the ferrite particles and the cationic nanogels that may assist the prevention of leakage of ferrite particles from the hydrogel matrix. The use of AAm as comonomer promotes the mechanical consistency of the hydrogel and gives the benefit of controlling charge distribution on the nanohydrogel systems. Therefore, for ferrite encapsulated cationic nanohydrogel composite synthesis, relatively higher amounts of crosslinker ratios, 3, 4, and a maximum of 5%, were used. When AAm was used as comonomer, relatively lower amounts of crosslinker ratio (1–2%) yield stable magnetic particles. When solely iron particles were prepared without any hydrogel encapsulating them, the color was bright and clear brown, in comparison with the whitish brown mixture of nanohydogel-encapsulated ferrite particles.

Figure 6a shows the TEM images of ferrite particles, and Fig. 6b shows the magnetic behavior or these particles after hydrogel coatings. Figure 6a clearly demonstrates that, without hydrogel coating, the sizes of ferrite particles are around 2–5 nm with distinctly seen lattice structures. The TEM images of iron particles after hydrogel coatings are presented in Fig. 7a. The TEM micrograph does not show very clear images of very small particles with hydrogel coatings; however, from the high-resolution image, Fig. 7b, ferrite lattices can be noticeable. It was confirmed with VSM results that the particles are superparamagnetic, which

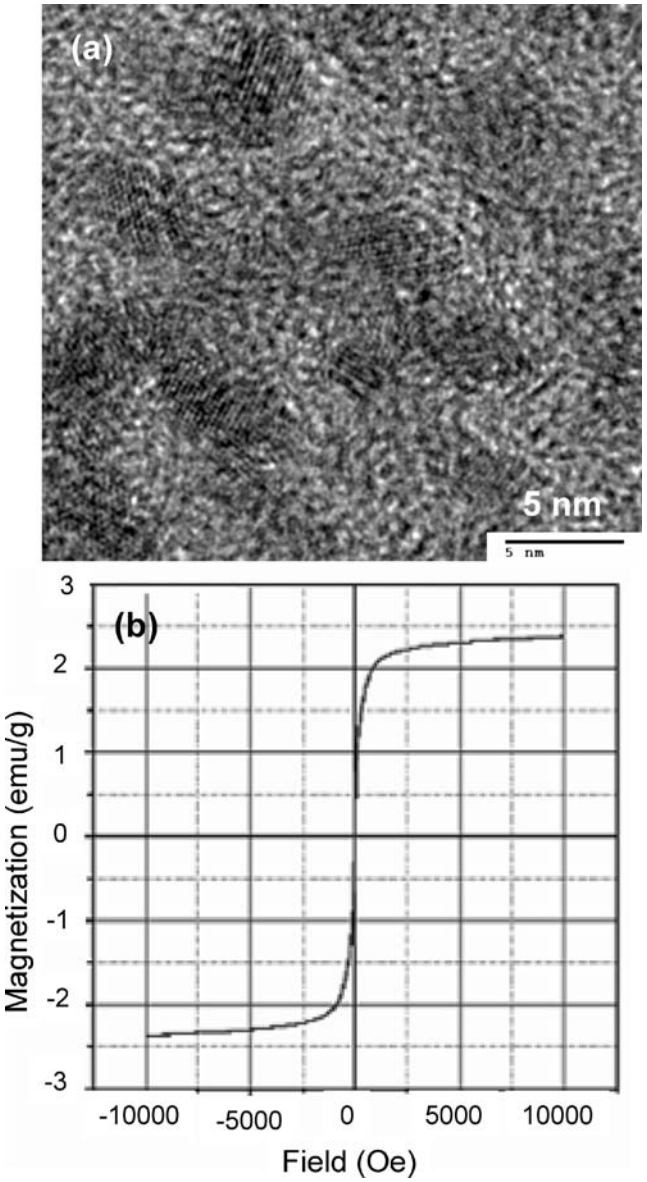

Fig. 6 **a** TEM images of ferrite particles. **b** Applied field vs magnetization plot of 4% X cationic hydrogels encapsulating ferrite particles obtained with VSM

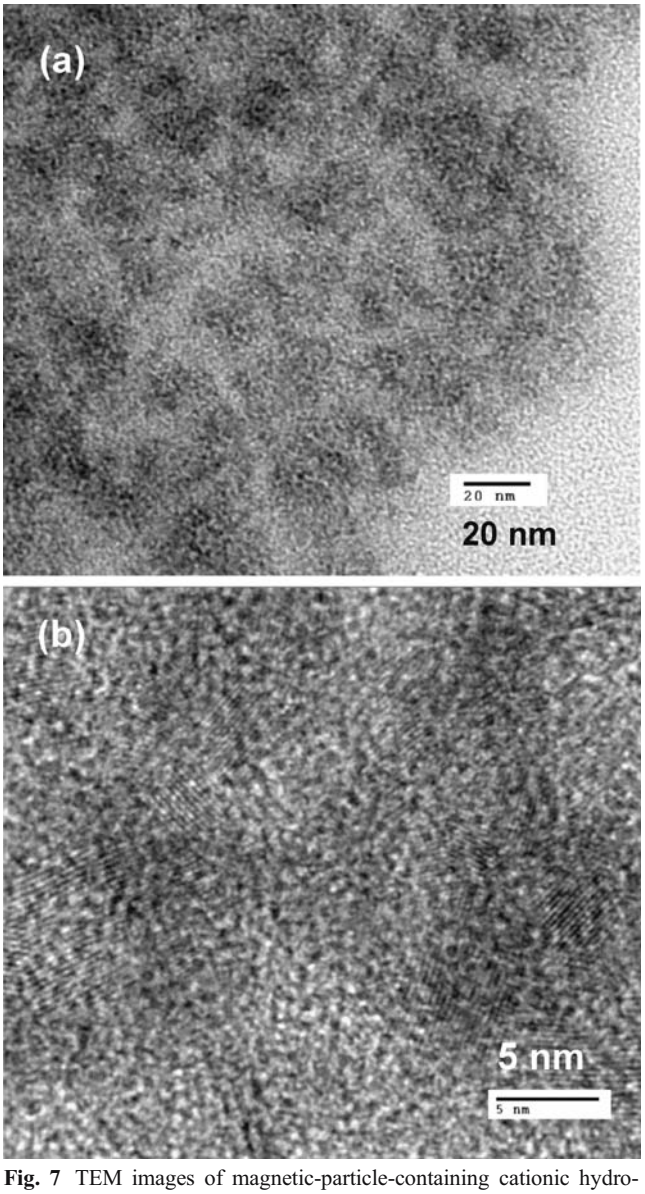

Fig. 7 TEM images of magnetic-particle-containing cationic hydrogels (**a**) and a close-up image (**b**)

is the case for magnetic particles less than 10 nm. It was reported that nanosize maghemite (~7 nm) containing biodegradable gel showed super paramagnetic behavior [44]. Figure 6b denotes the magnetic property of iron-encapsulated 4% X p(APTMACl) hydrogels, obtained via VSM measurements. As can be seen from the figure, after magnetization, composite particles have a room temperature magnetization of ~2.4 emu/g at 10 kOe, as determined by VSM. The absence of hysteresis at room temperature suggests completely superparamagnetic behavior consisting with the nanosize of ferrite particles; therefore, the composite material is magnetic-field-sensitive. In comparison with bulk magnetite or maghemite particles, these magnetic particle-containing hydrogel composites showed lower room-temperature magnetization, i.e., γ-Fe_2O_3 has saturation magnetization of around 60–80 emu/g at 300 K [44]. Here, the lower magnetization could be due to poorly crystalline magnetic nanoparticles, as well as to the formation of nonmagnetic phases of iron oxides. It is also possible that the interaction of ferrite particles with cationic hydrogel coating and/or the surface effect residual AOT in the magnetization of magnetic particles may result in reduced magnetization. Another possibility could be the smaller amount of magnetic particle in the nanocomposite structure.

These types of materials have many biological uses as controlled and guided delivery vehicles [29]. It is well known that polyelectrolyte complexes with oppositely charged species and, especially, cationic structures are useful in masking the negative charges of DNA, and have found immense applications such as in gene delivery [45–47].

Conclusions

With this investigation, it was shown that cationic hydrogel composites can be prepared in a variety of forms with additional functionalities utilizing the inverse micelle polymerization technique. The prepared nanosized hydrogels are very small (5–20 nm), highly charged, and predictably have faster response time, in comparison with bulk counterparts, to external stimuli such as pH, ionic strength, or a solute molecule. The additional functionalities established here are inorganic composites (pore size control and regulation, i.e., opening and closing in response to a stimulus and mechanical integrity as support) and magnetic field sensitivity with their tunable architectures provide additional advantages to hydrogels in their use in many field as carriers for sustained and uniform drug delivery devices, gene therapy, and biosensor applications. It was shown that these cationic nanohydrogels strongly bind to DNA [32]. The preparation of the magnetic particle coating with completely charged hydrogel shown in this investigation offer great potential on the guided delivery of active agents. Moreover, with their ceramic composites, material properties can be enhanced and unique architectures can be designed precisely to be applicable in pharmaceutical and biomedical fields, as well as sensor applications. As a result, hydrogels of nanosized materials with their composites have many viable applications in bio- and nanotechnology.

Acknowledgements The author is grateful to Prof. Dr. Vijay T. John for providing great contributions to the work. The author also acknowledges the Tulane Institute for Macromolecular Engineering and Science and the University of New Orleans for VSM measurements.

References

1. Takeoka Y, Watanabe M (2003) Adv Mater 15:1999
2. Konya Z, Puntes VF, Kiricsi I, Zhu J, Ager WJ, Ko KM, Frei H, Alivisatos P, Somorjai GA (2003) Chem Mater 15:1242
3. Landfester K (2001) Adv Mater 13:765
4. Kane RS, Cohen RE (1999) Chem Mater 11:90
5. Morimoto N, Endo T, Ohtomi M, Iwasaki Y, Akiyoshi K (2005) Macromol Biosci 5:710
6. Lu Z, Shutava T, Sahiner N, John V, Lvov Y (2005) Chem Lett 34:1536
7. Rohit G, Shutava T, Amish P, John VT, Lvov Y (2004) Macromolecules 37:4519
8. Jang J, Bae J (2005) Chem Commun 1200
9. Bharali DJ, Sahoo SK, Mozumdar S, Maitra A (2003) J Colloid Interface Sci 258:415
10. Hirai T, Watanabe T, Komasawa I (2000) J Phys Chem B 104:8962
11. Platonova OA, Bronstein LM, Solodovnikov SP, Yanovskaya IM, Obolonkova ES, Valetsky PM, Wenz E, Antonietti M (1997) Colloid Polym Sci 275:426
12. Eastoe J, Warne B (1996) Curr Opin Colloid Interface Sci 1:800
13. Peppas NA, Buresa P, Leobandung W, Ichikawab H (2000) Eur J Pharm Biopharm 50:27
14. Yong Q, Kinam P (2003) Adv Drug Deliv Rev 55:403
15. Kopeček J (2003) Eur J Pharm Biopharm 20:1
16. Yoshida R (2005) Curr Org Chem 9:1617
17. Hasegawa U, Nomura SM, Kaul SC, Hirano T, Akiyoshi K (2005) Biochem Biophys Res Comm 331:917
18. Kiser PF, Wilson G, Needham D (1998) Nature 30:459
19. Kataoka K, Miyazaki H, Bunya M, Okano T, Sakurai Y (1998) J Am Chem Soc 120:12694
20. Flynn L, Dalton PD, Shoichet SM (2003) Biomaterials 24:4265
21. Spohr R, Reber N, Wolf A, Alder GM, Ang V, Bashford CL, Pasternak CA, Omichi H, Yoshida M (1998) J Control Release 50:1
22. Shin Y, Chang JH, Liu J, Williford R, Shin YK, Exarhos GJ (2001) J Control Release 73:1
23. Hideko K, Tatsuo S, Eri A, Yoshikazu M, Akihiko K, Teruo O (2002) Anal Sci 18:45
24. Sun HW, Gong PJ, Liu XQ, Meng FZ, Wei XG, Hong J, Xu DM, Zhang CF, Wang YX, Yao SD (2005) Nucl Sci Tech 16:278
25. Kroll E, Winnik FM, Ziolo FR (1996) Chem Mater 8:1594
26. Pardo-Yissar V, Gabai R, Shipway AN, Bourenko T, Willner I (2001) Adv Mater 13:1320
27. Shipway AN, Willner I (2001) Chem Commun 20:2035
28. Lao LL, Ramanujan RV (2004) J Mater Sci Mater Med 15:1061
29. Liu TY, Hu SH, Liu TY, Liu DM, Chen SY (2006) Langmuir 22:5974
30. Wormuth K (2001) J Colloid Interface Sci 241:366

31. Juliac E, Mitsumata T, Taniguchi T, Iwakura K, Koyama K (2003) J Phys Chem B 107:5426
32. Sahiner N, Godbey WT, McPherson GL, John VT (2006) Colloid Polym Sci 284:1121
33. Li S, John VT, Irvin GC, Rachakonda SH, McPherson GL, O'Connor CJ (1999) J Appl Phys 85:5965
34. Isamu K, Atsushi S, Hideo N (2004) J Colloid Interface Sci 275:450
35. Essler F, Candau F (2001) Colloid Polym Sci 279:405
36. Braun O, Selb J, Canadu F (2001) Polymer 42:8499
37. McAllister K, Sazani P, Adam M, Cho MJ, Rubinstein M, Samulski RJ, DeSimone JM (2002) J Am Chem Soc 124:15198
38. Barton TJ, Bull LM, Klemperer WG, Loy DA, McEnaney B, Misono M, Monson PA, Pez G, Scherer GW, Vartuli JC, Yaghi OM (1999) Chem Mater 11:2633
39. Nagao D, Osuzu H, Yamada A, Mine E, Kobayashi Y, Konno M (2004) J Colloid Interface Sci 279:43
40. Fidalgo A, Rosa ME, Ilharco LM (2003) Chem Mater 15:2186
41. Itoh H, Sugimoto T (2003) J Colloid Interface Sci 265:283
42. Chatterjee J, Haik Y, Chen CJ (2003) J Magn Magn Mater 257:113
43. Sahiner N, Singh M, Kee DD, John VT, McPherson GL (2006) Polymer 47:1124
44. Chatterjee J, Haik Y, Chen JC (2003) Colloid Polym Sci 281:892
45. Vladimir SG, Olga NA, Olga PA, Anatoly ZA, Valentina RB, Alexander ZB, Kenichi Y, Victor KA (2002) J Am Chem Soc 124:11324
46. Rosso BA, Barbarisi M, Petillo O, Margarucci S, Calarco A, Peluso G (2003) Mater Sci Eng C Biomim Mater Sens Syst 23:371
47. Stefaan CDS, Joseph D, Wim HE (2000) Pharma Res 17:113